



Contents lists available at ScienceDirect

# Electrochemistry Communications

journal homepage: [www.elsevier.com/locate/elecom](http://www.elsevier.com/locate/elecom)



## Electrochemistry of 2-dimethylaminoethanethiol SAM on gold electrode: Interaction with SWCNT-poly(*m*-aminobenzene sulphonic acid), electric field-induced protonation–deprotonation, and surface $pK_a$

Jeseelan Pillay<sup>a</sup>, Bolade O. Agboola<sup>b</sup>, Kenneth I. Ozoemena<sup>b,\*</sup>

<sup>a</sup> Department of Chemistry, University of Pretoria, Pretoria 0002, South Africa

<sup>b</sup> Energy and Processes Unit, Materials Science and Manufacturing, Council for Scientific and Industrial Research (CSIR), Pretoria 0001, South Africa

### ARTICLE INFO

#### Article history:

Received 25 March 2009  
Received in revised form 20 April 2009  
Accepted 24 April 2009  
Available online xxx

#### Keywords:

Self-assembled monolayer  
Protonation-deprotonation  
Surface  $pK_a$   
Cyclic voltammetry  
Electrochemical impedance spectroscopy

### ABSTRACT

Electrochemical behaviour of self-assembled monolayer of 2-dimethylaminoethanethiol (DMAET) on gold electrode, with and without integration with SWCNT-poly(*m*-aminobenzene sulphonic acid) (SWCNT-PABS) has been probed. It is proved that the so-called electric field induced protonation–deprotonation process, hitherto observed for the –COOH terminated SAMs, is also observed for the –N(H)<sup>+</sup>(CH<sub>3</sub>)<sub>2</sub> terminated SAMs. The surface  $pK_a$  of DMAET was estimated as 7.6, smaller than its solution  $pK_a$  of 10.8. It is also shown that SWCNT-PABS is irreversibly attached to the DMAET SAM.

© 2009 Published by Elsevier B.V.

### 1. Introduction

Fabrication of ultrathin, well-ordered self-assembled monolayer (SAM) films of thiol-derived organic molecules on gold substrates has been a major research interests due to the potential ability of such ultrathin films to be used as scaffolds in a plethora of nanotechnological applications and fundamental studies including the immobilization of biomolecules (e.g., proteins, DNA) and redox-active functional materials for catalysis and sensing. For example, several potential applications of carbon nanotubes (CNTs) mean that some of their future applications in catalysis, sensing and electronics will require their integration on solid substrates as ultrathin nano-scaled molecular films. Self-assembled monolayers containing functional head groups (such as –COOH, –OH and –NH<sub>2</sub> head groups) that can easily be tuned by the bathing electrolyte solution are important and have been intensely studied. Knowledge of surface  $pK_a$  of SAM species is important for theoretical and potential applications of such SAMs [1–5]. More than a decade ago, Caruso et al. [6] reported the use of DMAET SAM as a platform for integrating DNA on gold surface. Since then, no work has been reported on this important SAM. Our laboratory has recently been engaged in interrogating the possibility of using

DMAET SAM as a potential base monolayer for forming multilayer films of metallophthalocyanine and SWCNT hybrids [7]. Successful future applications of this rarely studied DMAET SAM is dependent on thorough understanding of the state of the amino head group from which further surface functionality can be derived. In this communication, we used cyclic voltammetry (CV) and electrochemical impedance spectroscopy (EIS) to probe the behavior of the –N(CH<sub>3</sub>)<sub>2</sub> head group of DMAET SAM in solutions containing outer-sphere redox probe (K<sub>4</sub>Fe(CN)<sub>6</sub>/K<sub>3</sub>Fe(CN)<sub>6</sub>), different electrolytes and epinephrine.

SAMs with –COOH head groups exhibit reversible voltammetric behaviour due to the so-called electric field induced protonation/deprotonation effect rather than a Faradaic process [8–10]. For example, such process has been reported by White and co-workers for mercaptoundecanoic acid (MUA) SAMs on Ag(III) [8] and by Burgess and co-workers for MUA on polycrystalline gold [9] and 4-mercaptobenzoic acid (4-MBA) SAMs on polycrystalline gold bead electrode [10]. We prove for the first time that SAM with –N(H)<sup>+</sup>(CH<sub>3</sub>)<sub>2</sub> head group can also undergoes the electric field-induced protonation/deprotonation process [8–10], and that while this process can be irreversibly quenched by poly(*m*-aminobenzene sulphonic acid)-functionalised single-walled carbon nanotubes (SWCNT-PABS), it is reversibly quenched by large anions such as sulphate and perchlorate. Interestingly, we also show that the surface  $pK_a$  of DMAET is about 3  $pK_a$  lower than its bulk solution counterpart.

\* Corresponding author. Tel.: +27 12 841 3664; fax: +27 12 841 2135.  
E-mail address: [kozoemena@csir.co.za](mailto:kozoemena@csir.co.za) (K.I. Ozoemena).

## 2. Experimental

### 2.1. Materials and reagents

Single-walled carbon nanotube poly(*m*-aminobenzene sulfonic acid) (SWCNT-PABS) and 2-dimethylaminoethanethiol (DMAET) were obtained from Sigma–Aldrich. Sodium 2-mercaptoethanesulphonate (MES) was obtained from Merck. Ultra pure water of resistivity 18.2 MΩ cm was obtained from a Milli-Q Water System (Millipore Corp., Bedford, MA, USA) and was used throughout for the preparation of solutions. 0.01 M Phosphate buffer solutions (PBS) were prepared with appropriate amounts of K<sub>2</sub>HPO<sub>4</sub> and KH<sub>2</sub>PO<sub>4</sub>. A 5 mM K<sub>4</sub>Fe(CN)<sub>6</sub>/K<sub>3</sub>Fe(CN)<sub>6</sub> solution was prepared in PBS, pH adjusted appropriately with NaOH and HCl. All electrochemical experiments were performed with nitrogen-saturated PBS. All other reagents were of analytical grades and were used as received from the suppliers.

### 2.2. Apparatus and procedure

All electrochemical experiments were carried out using an Autolab Potentiostat PGSTAT 302 (Eco Chemie, Utrecht, The Netherlands) driven by the GPES and FRA softwares version 4.9. Electrochemical impedance spectroscopy (EIS) measurements were performed between 1.0 Hz and 10 kHz using a 5 mV rms sinusoidal modulation in a solution of 1 mM of K<sub>4</sub>Fe(CN)<sub>6</sub> and 1 mM K<sub>3</sub>Fe(CN)<sub>6</sub> (1:1) mixture containing 0.1 M KCl, and at the E<sub>1/2</sub> of the [Fe(CN)<sub>6</sub>]<sup>3-/4-</sup> (0.124 V vs. Ag|AgCl). Gold electrode (BAS, *r* = 0.8 mm) was used as the working electrode. Ag|AgCl, sat'd

KCl and platinum electrodes were used as reference and counter electrodes, respectively. All solutions were de-aerated by bubbling pure nitrogen (Afrox) prior to each electrochemical experiment. All experiments were performed at 25 ± 1 °C. AFM images were obtained at SAM-modified SPR gold disks (Eco-Chemie) using an AFM 5100 System (Agilent Technologies, AC mode AFM scanner interfaced with a PicoScan controller, scan range 1.25 μm in *x*-*y* and 2.322 μm in *z*, silicon type PPP-NCH-20 (Nanosensors®) of thickness 4.0 ± 1.0 μm, length 125 ± 10 μm, width 30 ± 7.5 μm, spring constants 10–30 N m<sup>-1</sup>, resonant frequencies of 204–497 kHz and tip height of 10–15 μm). All images (256 samples/line × 256 lines) were taken in air at room temperature and at scan rates 0.9–1.0 lines s<sup>-1</sup>.

### 2.3. Electrode modification and pretreatments

Polycrystalline gold electrode (BAS) was first cleaned by repetitive cyclic potential scanning between –0.25 and 1.5 V (vs. Ag|AgCl, sat'd KCl reference electrode) at a scan rate of 0.05 V s<sup>-1</sup> until a reproducible scan was obtained. The cleaned electrode was rinsed in both water and ethanol and then immersed in 4.5 mM DMAET ethanol solution for 18 h to form a monolayer (Au-DMAET). The p*K*<sub>a</sub> of DMAET is ~ 10.8 and expected to be positively charged [6]. The newly formed Au-DMAET electrode was rinsed in copious amount of distilled deionised water for 2 min. The formation SWCNT-PABS on the Au-DMAET was assembled by dipping the Au-DMAET electrode in a dispersion of SWCNT-PABS (1 mg SWCNT-PABS/1 ml PBS, pH 7.0) for 3.5 h. The electrode con-

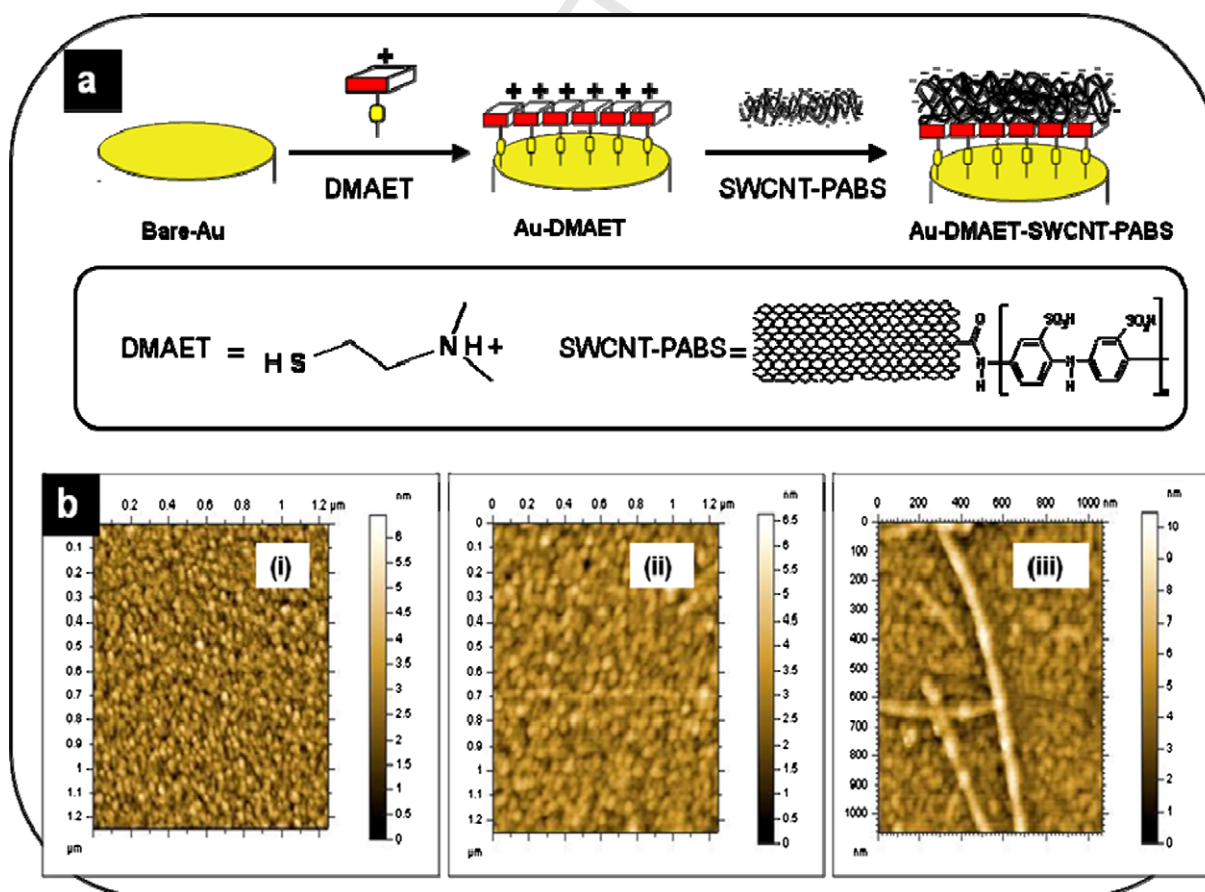


Fig. 1. (a) Cartoon showing the schematic representation of the SAM formation of DMAET and DMAET-SWCNT-PABS. (b) AFM images of corresponding (i) Bare-Au (ii) Au-DMAET and (iii) Au-DMAET-SWCNT-PABS.

131 taining SWCNT-PABS is herein referred to as **Au-DMAET-SWCNT-**  
132 **PABS**.

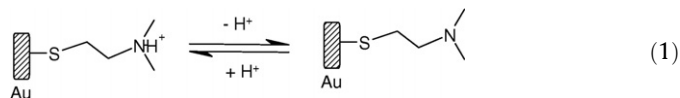
### 133 3. Results and discussion

#### 134 3.1. AFM characterization

135 Fig. 1a depicts the fabrication of DMAET SAM, while Fig. 1b  
136 shows the comparative AFM images of the (a) Bare-Au (b) Au-  
137 DMAET and (c) **Au-DMAET-SWCNT-PABS**. There was no significant  
138 difference between the thickness of the bare-Au and Au-DMAET,  
139 which is expected for this short-chained alkanethiol SAM as others  
140 [11] did not even observe any difference between bare Au and on  
141 modification with long-chained SAM of 11-amino-1-undecanethiol.  
142 The attachment of SWCNT-PABS is confirmed by the presence  
143 of the flat lying tubes on the surface of the DMAET molecules.

#### 144 3.2. Cyclic voltammetric behaviour in various electrolytes

145 Fig. 2a compares the CV of the three electrodes in PBS (pH 7.0).  
146 The reversible voltammogram for the Au-DMAET SAM is similar to  
147 those observed for mercaptoundecanoic acid (MUA) SAMs on  
148 Ag(III) [8] and on polycrystalline gold [9], and 4-mercaptobenzoic  
149 acid (4-MBA) SAMs on polycrystalline gold bead electrode [10],  
150 which the authors associated with the electric field induced proto-  
151 nation/deprotonation of the  $-\text{COOH}$  head groups rather than a  
152 Faradaic process. We believe that the same process is what is being  
153 observed in our case, i.e., electric field driven deprotonation/proto-  
154 nation of the  $-\text{N}(\text{H})^+(\text{CH}_3)_2$  head group of the DMAET (Eq. (1)):



156 Fig. 2a clearly suggests that the integration of the SWCNT-PABS  
157 via electrostatic interaction leads to suppression of the protona-  
158 tion-deprotonation process. To test this hypothesis, we conducted  
159 a series of experiments in different unbuffered electrolytes (50 mM  
160  $\text{K}_2\text{SO}_4$ , NaCl,  $\text{CaCl}_2$ , KCl, NaF and  $\text{KClO}_4$ ) with a view to establishing  
161 the impact of cations and anions on the evolution of this DMAET  
162 reversible voltammogram. As exemplified in Fig. 2b, unlike the  
163 NaF, and KCl that showed the same reversible process as the PBS,  
164  $\text{K}_2\text{SO}_4$  and  $\text{KClO}_4$  (not shown) suppressed the Au-DMAET volta-  
165 mmogram. Repetitive scanning in any of the electrolyte showed stable  
166 voltammograms (exemplified in Fig. 2c with NaF). It may be  
167 inferred from the CVs that (i) the appearance of the reversible  
168 peaks in chloride and non-chloride solutions (PBS and NaF) rules  
169 out this possibility adsorption/desorption of chloride ions being  
170 responsible for the peaks; (ii) cations do not have any impact con-  
171 trary to the report of Rosentahl and Burgess on 4-MBA [10], and  
172 (iii) anions have impact but possibly depend on the size of anion;  
173  $\text{SO}_4^{2-}$  and  $\text{ClO}_4^-$  are approximately of the same size and larger than  
174  $\text{Cl}^-$  that did not show any impact. Unlike the SWCNT-PABS, the ori-  
175 ginal voltammogram can be regenerated when re-immersed in KCl  
176 solution (Fig. 2b), meaning that SWCNT-PABS is irreversibly ad-  
177 sorbed onto the DMAET while the anions are weakly adsorbed.  
178 Also, we examined the CV of the SAM of MES (same structure as  
179 DMAET, differing only in the head group) and did not observe  
180 any peak in the PBS (not shown), which confirms that the revers-  
181

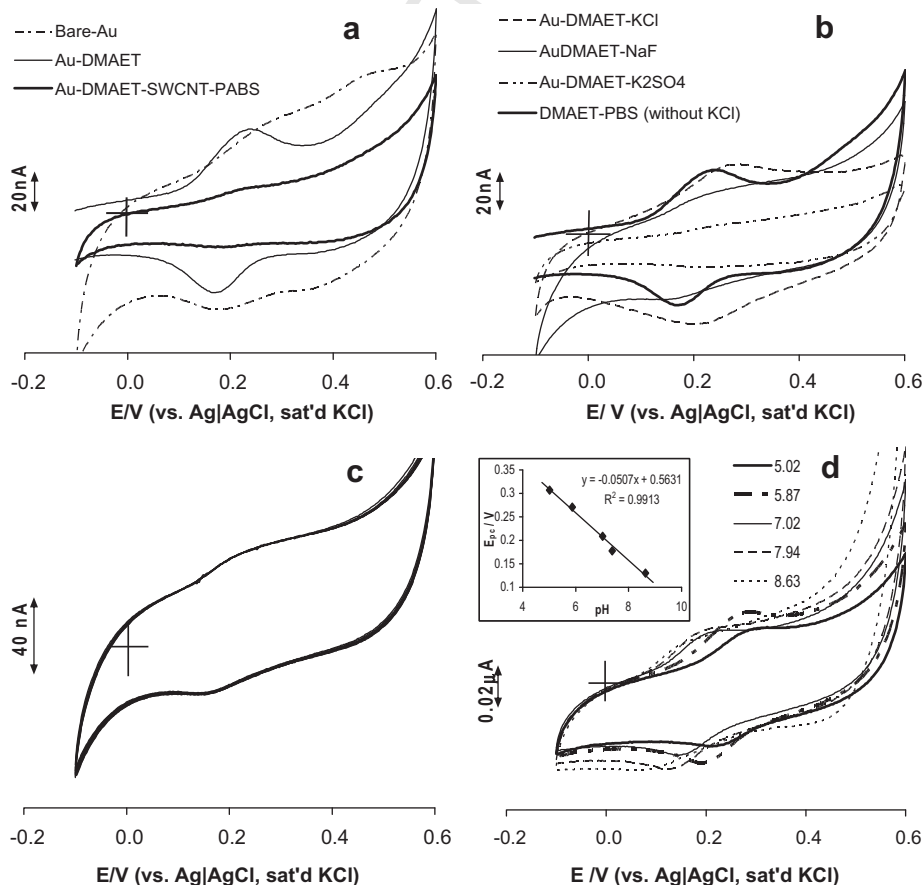


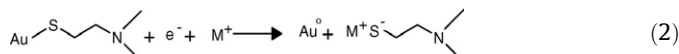
**Fig. 2.** Typical cyclic voltammetric evolutions of (a) Bare-Au, Au-DMAET and Au-DMAET-SWCNT-PABS in PBS pH 7.4; (b) shows the Au-DMAET in 50 mM PBS, NaF, KCl and  $\text{K}_2\text{SO}_4$ ; (c) repetitive cycling of Au-DMAET in 50 mM NaF; and (d) in phosphate buffer solutions at different pHs. All CV measurements were recorded at  $0.025 \text{ Vs}^{-1}$  scan rates.

Please cite this article in press as: J. Pillay et al., Electrochemistry of 2-dimethylaminoethanethiol SAM on gold electrode: Interaction with SWCNT-poly(*m*-aminobenzene sulphonic acid), electric field-induced protonation-deprotonation, and surface  $\text{pK}_a$ , *Electrochem. Commun.* (2009), doi:10.1016/j.elecom.2009.04.028



ible peaks in DMAET SAM arise from its amino head group. Furthermore, the behavior of the observed peak was also studied in PBS at different pH values. Fig. 2d shows that the position of the peak potentials shifted as a function of the electrolyte's pH with a slope of *ca.* – 51 mV/decade. The discrepancy from the ideal 59 mV/decade may be because we are plotting the applied electrode potential rather than the local potential,  $\Psi$ , according to the Smith and white model [12].

Next, we performed cyclic voltammetric reductive desorption experiment in 0.5 M KOH between 0 and –1.2 V (vs. Ag|AgCl sat'd KCl), Eq. (2) representing the chemistry of such irreversible desorption of the DMAET SAM:



where  $\text{M}^+$  represents the cation from the electrolyte [13]. The same equation holds for the DMAET–SWCNT–PABS. We observed the sharp desorption peaks (CV not shown) at –0.72 V and –0.68 V for DMAET and DMAET–SWCNT–PABS, respectively. From the area (i.e., charge,  $Q/C$ ) under the respective reductive peaks, the surface concentrations ( $\Gamma_{\text{SAM}}/\text{mol cm}^{-2}$ ) of the DMAET and DMAET–SWCNT–PABS were estimated from Eq. (3):

$$\Gamma_{\text{SAM}} = \frac{Q}{nFA} \quad (3)$$

where symbols retain their conventional meaning. The  $\Gamma_{\text{SAM}}$  was approximately  $0.53 \text{ nmol cm}^{-2}$  for DMAET and  $0.58 \text{ nmol cm}^{-2}$  for the DMAET–SWCNT–PABS. This similar surface coverage for both SAMs suggests that the observed electrochemistry was due to SWCNT–PABS attached onto the surface of the DMAET molecules.

### 3.3. Electron transfer dynamics: Surface $pK_a$ of immobilized DMAET

The charge transfer resistance ( $R_{\text{ct}}$ ) values, extracted from the impedance spectra using the “find circle” method of the FRA software, decreased as Au–DMAET (12) < Au–DMAET–SWCNT–PABS (115) < bare Au (730). The slightly faster electron transfer recorded at the Au–DMAET compared to the Au–DMAET–SWCNT–PABS is attributed to the strong electrostatic attraction between the positively charged DMAET and the negatively charged  $[\text{Fe}(\text{CN})_6]^{3-/4-}$  species.

The  $pK_a$  of the surface-confined species is the value of the pH in contact with monolayer when half of the functional groups are ionized [5,14,15]. Fig. 3a represents typical impedance spectral profiles of Au–DMAET in PBS solutions of  $[\text{Fe}(\text{CN})_6]^{3-/4-}$ . Increase in solution pH from ~4.5 to 9.0 clearly depicts changes in electron transport, signified by increasing  $R_{\text{ct}}$  values (Fig. 3). At low pH (< pH 7.0), the  $-\text{N}(\text{H})^+(\text{CH}_3)_2$  head group is mostly protonated (reverse reaction of Eq. (3) favoured) thereby enhancing electrostatic attraction between the Au–DMAET and the negatively charged  $[\text{Fe}(\text{CN})_6]^{3-/4-}$  redox probe. However, increase in solution of pH > 7.0 leads to an increase in  $R_{\text{ct}}$  caused by deprotonation process (forward reaction of Eq. (2) favoured) resulting in electrostatic repulsion between the DMAET head group and the redox probe. From the mid-points of the  $R_{\text{ct}}$  vs. pH plots (Fig. 3b), the surface  $pK_a$  of the DMAET was estimated as ~7.6, which is about 3  $pK_a$  units lower than its solution  $pK_a$  of 10.8 [6]. The reason for this large shift of  $pK_a$ , as opposed to the usual order of <1  $pK_a$  is not understood at this time. However, our result is similar to the observation of Saby et al. [16] who reported a shift of the  $pK_a$  of benzoic acid from a value of 4.2 in solution to a value of 2.8 when covalently attached onto a glassy carbon electrode, which they speculated to be due to some specific interfacial effect between the carbon surface and the carboxylate functionalities or the phenyl ring of the layer. On the other hand, Abinam et al. [17] who also observed such large shifts in benzoic acid proved this to be due to

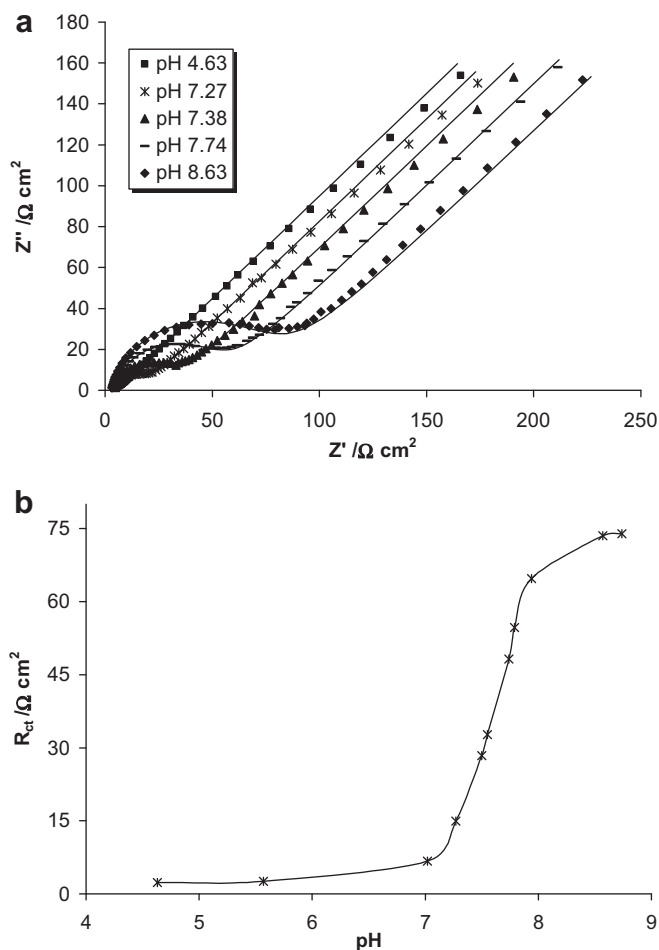


Fig. 3. (a) Examples of the impedimetric responses of the Au–DMAET at the different pH of  $[\text{Fe}(\text{CN})_6]^{3-}/[\text{Fe}(\text{CN})_6]^{4-}$  solutions, and (b) the corresponding plot of charge transfer resistance ( $R_{\text{ct}}$ ) vs. solution pH.

some thermodynamic factors. Also, interestingly, Abinam et al. [18] observed a large shift in the  $pK_a$  of “Jeffamine” from a value of 9.7 in solution to a value of 7.1 when covalently attached onto a carbon substrate and attributed that to entropic contribution arising from the ordering/disordering of solvent molecules at the carbon–water interface. Thus, we may conclude that our results may be connected with some specific interfacial effect between the DMAET and the gold surface or thermodynamic effects playing some interesting role.

## 4. Conclusion

Electrochemical properties of DMAET SAM, with and without integration with SWCNT–PABS have been probed. A well-defined reversible voltammetry observed for the DMAET SAM is ascribed to electric field-induced protonation–deprotonation of the  $-\text{N}(\text{H})^+(\text{CH}_3)_2$  head group rather than a Faradaic process., phenomenon hitherto observed for the  $-\text{COOH}$  terminated SAMs. We show that SWCNT–PABS is irreversibly attached to the DMAET. The surface  $pK_a$  of DMAET is about 7.6, about 3  $pK_a$  units less than its solution  $pK_a$ .

## Acknowledgements

We thank NRF (GUN # 2073666, 65305, 68338) for their support. J.P. thanks Mintek for Ph.D. scholarship.

266  
267  
268  
269  
270  
271  
272  
273  
274  
275  
276  
277

References

[1] K.I. Ozoemena, D. Nkosi, J. Pillay, *Electrochim. Acta* 53 (2008) 2844.  
[2] M.A. Bryant ad, R.M. Crooks, *Langmuir* 9 (1993) 385.  
[3] J. Zhao, L. Luo, X. Yang, E. Wang, S. Dong, *Electroanalysis* 11 (1999) 1108.  
[4] M. Root, A.M. Shaw, *Phys. Chem. Chem. Phys.* 8 (2006) 4741.  
[5] T.R. Lee, R.D. Carey, H.A. Biebuyck, G.M. Whitesides, *Langmuir* 10 (1994) 741.  
[6] F. Caruso, E. Rodda, D.N. Furlong, V. Haring, *Sensor Actuat. B* 41 (1997) 89.  
[7] J. Pillay, K.I. Ozoemena, *Electrochim. Acta*, in press, doi:10.1016/j.electacta.2008.12.056.  
[8] H.S. White, J.D. Peterson, Q. Cui, K.J. Stevenson, *J. Phys. Chem. B* 102 (1998) 2930.  
[9] I. Burgess, B. Seivewright, R.B. Lennox, *Langmuir* 22 (2006) 4420.

[10] S.M. Rosenthal, I.J. Burgess, *Electrochim. Acta* 53 (2008) 6759.  
[11] J.M. Campiña, A. Martins, F. Silva, *J. Phys. Chem. C* 111 (2007) 5351.  
[12] C.P. Smith, H.S. White, *Langmuir* 9 (1993) 1.  
[13] H.O. Finklea, in: A.J. Bard, I. Rubinstein (Eds.), *Encyclopedia Chemistry*, vol.19, Marcel Dekker, New York, 1996, pp. 109–335.  
[14] D. Nkosi, K.I. Ozoemena, *Electrochim. Acta* 53 (2008) 2782.  
[15] B.O. Agboola, K.I. Ozoemena, *Phys. Chem. Chem. Phys.* 10 (2008) 2399.  
[16] C. Saby, B. Ortiz, G.Y. Champagne, D. Bèlanger, *Langmuir* 13 (1997) 6805.  
[17] P. Abiman, A. Crossley, G.G. Wildgoose, J.H. Jones, R.G. Compton, *Langmuir* 23 (2007) 7847.  
[18] P. Abiman, G.G. Wildgoose, A. Crossley, J.H. Jones, R.G. Compton, *Chem. Eur. J.* 13 (2007) 9663.

278  
279  
280  
281  
282  
283  
284  
285  
286  
287  
288  
289  
290

UNCORRECTED PROOF